Polymer 50 (2009) 5653–5660

Contents lists available at ScienceDirect

Polymer

journal homepage: www.elsevier.com/locate/polymer

Soluble semi-conductive chelate polymers containing Cr(III) in the backbone: Synthesis, characterization, optical, electrochemical, and electrical properties

Mehmet Yıldırım, İsmet Kaya*

Çanakkale Onsekiz Mart University, Faculty of Sciences and Arts, Department of Chemistry, TR-17020 Çanakkale, Turkey

ARTICLE INFO

Article history:
Received 13 April 2009
Received in revised form
12 June 2009
Accepted 16 June 2009
Available online 27 June 2009

Keywords:
Chelate polymers
Metallopolymers
Conjugated polymers

ABSTRACT

Soluble kinds of coordination polymers containing Cr(III) ion in the backbone were synthesized. Structures of the polymers were characterized by FT-IR, UV–vis, ^{1}H and ^{13}C NMR, and size exclusion chromatography (SEC). Thermal degradation data were obtained by TG–DTA and DSC techniques. Cyclic voltammetry (CV) measurements were carried out and the HOMO–LUMO energy levels and electrochemical band gaps (E_g') were calculated. Additionally, the optical band gaps (E_g) were determined by using UV–vis spectra of the materials. Electrical conductivity measurements of doped (with iodine) and undoped polymers related to temperature were carried out by four-point probe technique using a Keithley 2400 electrometer. Measurements were made by using the polymeric films deposited on ITO glass plate by dip-coating method. Also, absorption spectra of doped polymeric films were recorded by a single beam spectrophotometer showing that doping procedure causes shifting in absorption spectra. Their abilities of processing in gas sensors were also discussed. According to obtained results the synthesized chelate polymers are semi-conductors having polyconjugated structures. Also, P-2 is the most electro-conductive polymer among the synthesized, while P-1 is the most thermally stable one.

1. Introduction

Imine polymers and their derivatives have been previously studied for their thermal, electrical, electrochemical, and optical properties [1–4]. Moreover, some of the oligophenol derivatives of Schiff base compounds have been used as antimicrobial agents [5]. For example, polyazomethines (PAMs) that have π-conjugated systems have low band gaps and, consequently, have semiconductivities [6–8].

Over the past several decade metal-containing polymers, especially their liquid crystalline materials have attracted considerable attention owing to their unusual properties [9,10]. The presence of metals in polymeric materials leads to new physical properties and potential applications. Kelch and Rehahn synthesized well-characterized ruthenium based coordination polymers [11,12]. Swager et al. investigated cobalt containing conducting metallopolymers for nitric oxide gas sensing [13]. Whittell and Manners reviewed metallopolymers as new multifunctional materials. This review surveys the range of application fields of chelate polymers including the use of conductive–semi-conductive materials, photo and electroluminescent materials, photovoltaic materials, liquid crystalline materials, catalysis and electrocatalysis, etc. [14]. Also, Archer emphasized that syntheses of linear metal coordination polymers through functionalized metal coordination monomers copolymerized by polymerization reactions on the organic part of the molecules often provide higher molecular weight species than syntheses using metal salts plus bridging ligands [15].

We previously synthesized many kinds of coupling transition metal complexes formed by binding metal ion to π-conjugated polymers and oligomers to hybrid material [16–19]. In this approach, the polymer or oligomer acts as a ligand to the metal. Common properties of these polymers are low solubility, high thermal stability, and shifting in absorbance spectrum allowing using in optical and sensing materials. Researchers have investigated several active groups in this field such as metal functionalized polyanilines [20], poly(phenyleneethylene) derivatives containing metals [21], luminescent transition metal-containing polymers [22], etc.

Metal-containing conjugated oligomers and polymers have been previously reviewed by Wolf [23] and three model systems to synthesize these polymers were shown as in Scheme 1. Also, it was stressed that most of unfunctionalized polymers suffer from poor solubility and consequently it is harder to characterize these polymers if sample is needed as a solution form.

In the literature, three possible methods have been suggested to obtain metal coordination polymers [24]: In the first method, preformed metal complexes are polymerized through functional

* Corresponding author. Tel.: +90 286 218 00 18; fax: +90 286 218 05 33.
E-mail address: kayaismet@hotmail.com (İ. Kaya).

0032-3861/$ – see front matter © 2009 Elsevier Ltd. All rights reserved.
doi:10.1016/j.polymer.2009.06.053

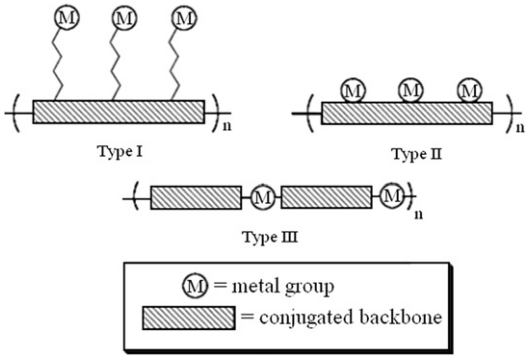

Scheme 1. Model systems of chelate polymers.

groups where the polymer forming step is a condensation or an addition reaction. The second method includes coordination of a metal ion by a preformed polymer containing chelating groups. In the last method, metal coordination polymer is formed via coordination reaction of a ligand which can attach itself simultaneously to two metal atoms or ions. The synthesis procedure used in this study is like the first method and it is seen that the obtained polymers are like Type III as shown in Scheme 1.

We previously investigated the effect of metal type on solubility of chelate polymers and we reported that Cr(III) containing chelate polymers have higher solubility among the synthesized (Cu, Co, Pb, Ni, Zn, Cd, Mn, Zr, Cr containing kinds) [25]. Also, we reported that these kinds of chelate polymers have reasonable electrical conductivity depending on low band gap and they have potential use in electronic, optoelectronic, photovoltaic, or electroactive applications. In this study we synthesized new soluble chelate polymers having polyconjugated structures. Cr(III) salt was used to obtain soluble kinds of chelate polymers. We characterized the polymers using FT-IR, UV–vis, and ^{1}H NMR, ^{13}C NMR, SEC, TG–DTA, and DSC techniques. We also determined optical and electrochemical properties of the polymers. In addition, electrical conductivities of doped and undoped polymers related to doping time and temperature have been measured by four-point probe technique at atmospheric pressure.

2. Experimental

2.1. Materials

3,4-Dihydroxybenzaldehyde, $CrCl_3 \cdot 6H_2O$, *o*-phenylenediamine, *p*-phenylenediamine, naphthalene-1,5-diamine, methanol, acetonitrile, chloroform, dimethylformamide (DMF), dimethylsulfoxide (DMSO), and tetrabutylammonium hexafluorophosphate ($TBAPF_6$) were supplied from Merck Chemical Co. (Germany) and they were used as received.

2.2. Syntheses of the polymers

The synthetic routes of the novel chelate polymers are shown in Scheme 2. The synthesis procedure contains two steps: The first step consists of coordination reaction of 3,4-dihydroxybenzaldehyde (3,4-HBA) with Cr(III) ion to form Cr-coordinated dialdehyde molecule (monomeric model compound-3,4-HBA-Cr). The second step consists of polymer forming which is a simple polycondensation reaction occurs between different aromatic diamine compounds with preformed to obtain Cr-coordinated polyazomethine kinds. Reactions were made as follow: 3,4-HBA (1.38 g, 1×10^{-2} mol) was placed into a 250 mL three-necked round-bottom flask which was fitted with condenser, thermometer and magnetic stirrer. 50 mL methanol was added into the flask and reaction mixture was heated at 60 °C. A solution of $CrCl_3 \cdot 6H_2O$ (1.86 g, 0.7×10^{-2} mol) in 30 mL methanol was added into the flask and reaction mixture was mixed one hour under reflux. Then, a solution of *o*-phenylenediamine (OPDA) (0.54 g, 0.5×10^{-2} mol), *p*-phenylenediamine (PPDA) (0.54 g, 0.5×10^{-2} mol) or naphthalene-1,5-diamine (NDA) (0.79 g, 0.5×10^{-2} mol) in 30 mL methanol was added into the flask. Reactions were maintained for 3 h under reflux. Polymers were precipitated by dropping into 250 mL toluene. Obtained polymers were washed with toluene (2×100 mL) and water (2×100 mL), respectively, and dried in vacuum oven for 24 h.

2.3. Characterization techniques

The solubility tests were done in different solvents by using 1 mg sample and 1 mL solvent at 25 °C. The infrared and ultraviolet–visible spectra were measured by Perkin Elmer FT-IR Spectrum one and Perkin Elmer Lambda 25, respectively. The FT-IR spectra were recorded using universal ATR sampling accessory (4000–550 cm^{-1}). ^{1}H and ^{13}C NMR spectra (Bruker AC FT-NMR spectrometer operating at 400 and 100.6 MHz, respectively) were also recorded by using deuterated DMSO-d_6 as a solvent at 25 °C. Tetramethylsilane was used as internal standard. Thermal data were obtained by using a PerkinElmer Diamond Thermal Analysis system. TG–DTA measurements were made between 20 and 1000 °C (in N_2, rate 10 °C/min). DSC analyses were carried out by using Perkin Elmer Pyris Sapphire DSC. DSC measurements were made between 25 and 420 °C (in N_2, rate 20 °C/min). The number-average molecular weight (M_n), weight average molecular weight (M_w), and polydispersity index (PDI) were determined by size exclusion chromatography (SEC) techniques of Shimadzu Co. For SEC investigations an SGX (100 Å and 7 nm diameter loading material) 3.3 mm i.d. × 300 mm column was used; eluent: DMF (0.4 mL/min), polystyrene standards. A refractive index detector (RID) and UV detector were used to analyze the products at 25 °C.

2.4. Optical and electrochemical properties

Ultraviolet–visible (UV–vis) spectra were measured by Perkin Elmer Lambda 25. The absorption spectra were recorded by using MeOH at 25 °C. The optical band gaps (E_g) were calculated from their absorption edges.

Cyclic voltammetry (CV) measurements were carried out with a CHI 660 °C Electrochemical Analyzer (CH Instruments, Texas, USA) at a potential scan rate of 20 mV/s. All the experiments were performed in a dry box filled with argon at room temperature. A platinum working electrode, Ag wire as reference electrode, and platinum wire as counter electrode were used. The electrochemical potential of Ag was calibrated with respect to the ferrocene/ferrocenium (Fc/Fc^+) couple. The half-wave potential ($E^{1/2}$) of (Fc/Fc^+) measured in acetonitrile solution of 0.1 M tetrabutylammonium hexafluorophosphate ($TBAPF_6$) and was 0.39 V with respect to Ag wire. The voltammetric measurements were carried out in DMSO/acetonitrile mixture (v/v, 1/4). The HOMO–LUMO energy levels and electrochemical band gaps (E'_g) were calculated from oxidation and reduction onset values [7].

2.5. Electrical properties

Polymer films were prepared on indium-tin-oxide (ITO) glass plate by dip-coating technique using a KSV Dip Coater instrument. The process has been carried out by successive dipping and

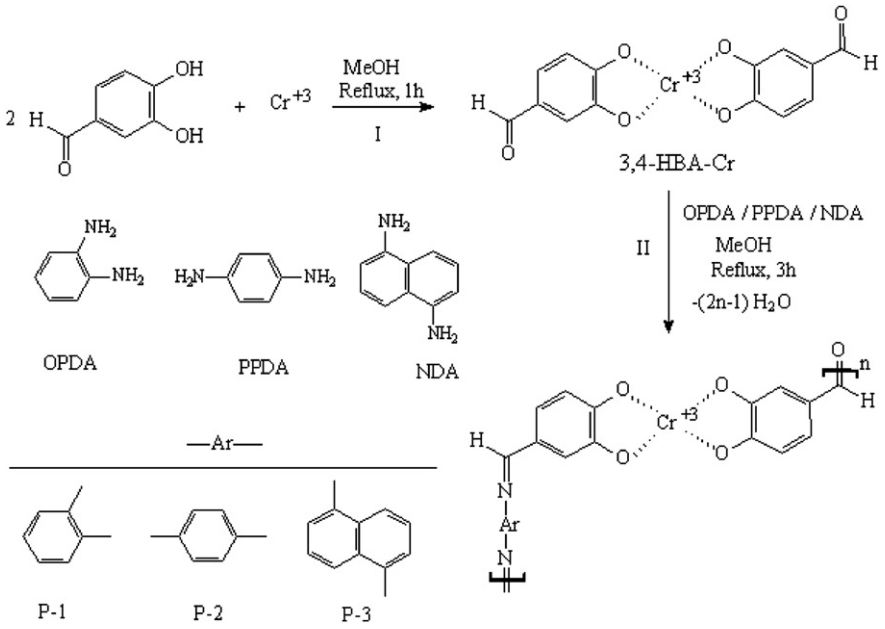

Scheme 2. Syntheses of the polymers.

withdrawal of ITO glass plate in a homogenous solution of P-1, P-2, and P-3 in methanol (50 mg/mL for each solution) for 50 times. After each dipping the films were kept for 1 min for drying [26].

Conductivities of the synthesized polymers were measured on a Keithley 2400 Electrometer, using four-point probe technique. Instrument was calibrated with ITO glass plate. Iodine doping was carried out by exposure of the polymer films to iodine vapor at atmospheric pressure in a desiccator [25]. Measurements were carried out at various temperatures between 20 and 80 °C.

Absorption spectra of the doped polymer films were measured by "Analytikjena Specord S 600" single beam spectrophotometer.

3. Results and discussion

3.1. Solubility and structures

The synthesized chelate polymers have considerable solubilities in common organic solvents. P-1 and P-3 are completely soluble in polar solvents such as DMSO, DMF, and methanol at 25 °C, whereas P-2 is partly soluble at the same temperature. However, it is completely soluble in DMSO and DMF at higher temperatures. All are insoluble in acetonitrile and chlorinated solvents such as CCl_4, $CHCl_3$, and CH_2Cl_2, even with heating.

The FT-IR spectral data are summarized in Table 1. As seen in Table 1, the structures of the synthesized polymers are confirmed by growing new peaks at about 650–660 cm^{-1} and 1600–1630 cm^{-1} indicating Cr(III)–O coordination bond and imine (CH═N) bond, respectively [25]. These changes are also shown in Fig. 1. The peaks at 1632–1649 cm^{-1} indicate aldehyde groups at the terminal positions of the polymers. However, completely disappearing of amine groups of OPDA, PPDA and NDA after polycondensation reactions shows that the synthesized polymers probably contain two aldehyde groups in two sides. Additionally, –OH peaks observed in these spectra can be attributed to absorbed and/or hydrate water, which is also confirmed by TG and DSC analyses, as explained below.

^{1}H–^{13}C NMR spectra of P-2 and P-3 are given in Figs. 2 and 3, respectively. According to ^{1}H NMR spectra, because of the paramagnetic structures of Cr(III) species the broad peaks are observed. As seen in Fig. 2a, P-2 has terminal aldehyde groups at 10.15 ppm, and imine peak is observed at 9.64 ppm. Also, at the ^{13}C NMR spectra of P-2, the peak values of aldehyde and imine carbons are at 191.59 and 160.00 ppm, respectively. As shown below, terminal aldehyde groups and imine protons of P-3 are also observed at 10.28 and 9.71 ppm, respectively. Also, at the ^{13}C NMR spectra of P-

Table 1
FT-IR analysis results of the synthesized compounds.

Compounds	Wavenumber (cm^{-1})					
	–OH	C–H (aromatic)	HC═O (terminal)	CH═N	C═C (aromatic)	M–O
P-1	3349	3047	1649	1630	1582, 1498, 1484	662
P-2	N.D[a]	3039	1639	1603	1581, 1490, 1452	657
P-3	N.D[a]	3035	1632	1605	1575, 1487, 1450	655

[a] N.D, not determined.

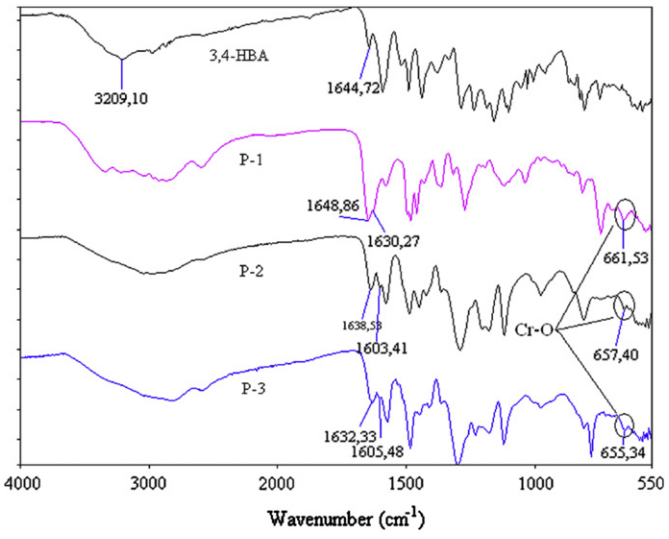

Fig. 1. FT-IR spectra of 3,4-dihydroxybenzaldehyde (3,4-HBA), P-1, P-2, and P-3.

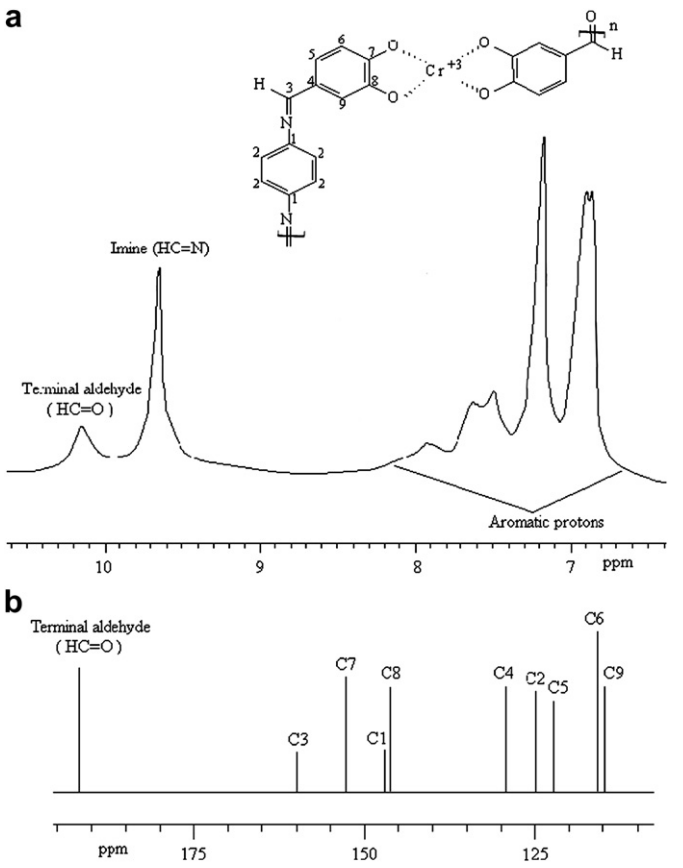

Fig. 2. ^{1}H NMR spectra (a) and ^{13}C NMR spectra (b) of P-2 obtained in DMSO.

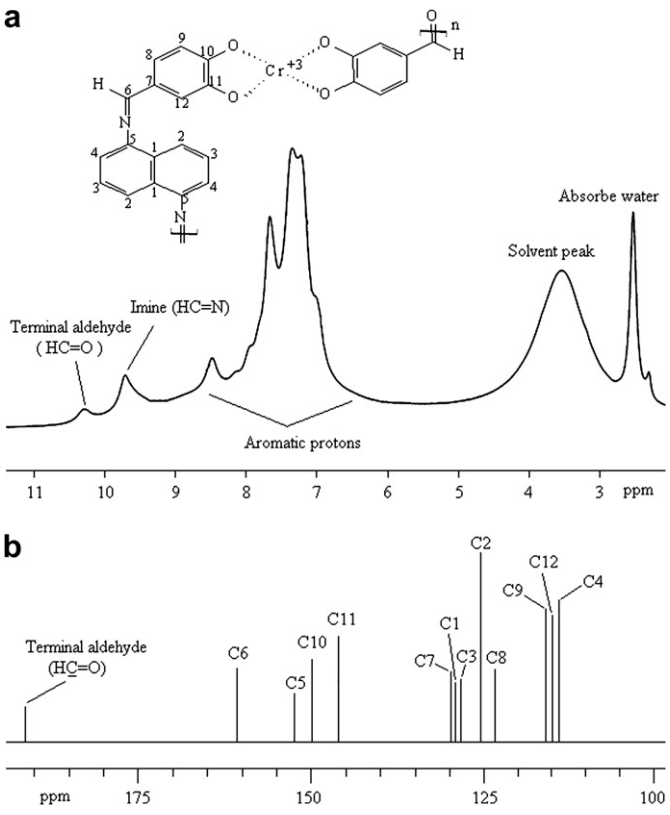

Fig. 3. ^{1}H NMR spectra (a) and ^{13}C NMR spectra (b) of P-3 obtained in DMSO.

3, the peak values of terminal aldehyde and imine carbons are at 191.25 and 160.16 ppm, respectively. These results confirm the presented structures of the synthesized chelate polymers. The other NMR analysis results of P-2 and P-3 were found as follows:

P-2: ^{1}H NMR (DMSO)/δ ppm: 10.15 (s, terminal aldehyde, HC═O), 9.64 (s, –CH═N–), 6.80–8.30 (m, aromatic). ^{13}C NMR (DMSO)/δ ppm: 191.59 (terminal aldehyde, HC═O), 160.00 (C3–H), 152.64 (C7-ipso), 147.09 (C1-ipso), 146.38 (C8-ipso), 129.29 (C4-ipso), 124.92 (C2–H), 122.26 (C5–H), 116.04 (C6–H), 114.91 (C9–H).

P-3: ^{1}H NMR (DMSO)/δ ppm: 10.28 (s, terminal aldehyde, HC═O), 9.71 (s, –CH═N–), 6.80–8.70 (m, aromatic). ^{13}C NMR (DMSO)/δ ppm: 191.25 (terminal aldehyde, HC═O), 160.16 (C3–H), 152.34 (C5-ipso), 149.84 (C10-ipso), 146.09 (C11-ipso), 129.84 (C7-ipso), 129.22 (C1-ipso), 128.28 (C3–H), 125.47 (C2–H), 123.28 (C8–H), 115.94 (C9–H), 114.84 (C12–H), 113.28 (C4–H).

3.2. Size exclusion chromatography

According to SEC chromatograms, the calculated number-average molecular weight (M_n), weight average molecular weight (M_w), and polydispersity index (PDI) values measured using both of RI and UV detectors are given in Table 2. According to these results P-1, P-2, and P-3 contain approximately 24–27, 21–22, and 26–32 repeated units, respectively. These results confirm the polymeric structures of the synthesized compounds. These results also agree with previous studies [25].

3.3. Optical and electrochemical properties

Cyclic voltammograms of the synthesized polymers are shown in Fig. 4a. According to cyclic voltammetry (CV) measurements P-1, P-2, and P-3 are oxidized at 1.39, 1.43, and 1.41 V, respectively. Also, the reduction peaks are obtained at −0.89, −0.55, and −0.73 V for P-1, P-2, and P-3, respectively. HOMO–LUMO energy levels and electrochemical band gaps (E'_g) were calculated by using the following equations [27] and given in Table 3.

$$E_{HOMO} = -(4.39 + E_{ox}) \quad (1)$$

$$E_{LUMO} = -(4.39 + E_{red}) \quad (2)$$

$$E'_g = E_{LUMO} - E_{HOMO} \quad (3)$$

where E_{ox} is the oxidation peak potential and E_{red} is the reduction peak potential.

The HOMO–LUMO energy levels and electrochemical band gaps are also shown schematically in Fig. 4b. According to obtained results the order of electrochemical band gap values of the polymers changes as follow: P-2 < P-3 < P-1.

The UV–vis spectrum of the model compound and the polymers exhibit absorbances (λ_{max}) at 214, 253, 336, and 404 nm for 3,4-HBA-Cr, 209, 234, 276, 375, and 453 nm for P-1, 208, 231, 275, and 467 nm for P-2, and 212, 244, 338 and 452 nm for P-3. The R-bands observed at 404, 453, 467, and 452 nm for 3,4-HBA-Cr, P-1, P-2 and

Table 2
SEC analysis results of the synthesized polymers.

Compounds	Molecular weight distribution values					
	RI detector			UV detector		
	M_n	M_w	PDI	M_n	M_w	PDI
P-1	10 700	12 700	1.187	9500	11 050	10 163
P-2	8800	8950	1.017	8600	8800	1.023
P-3	11 700	18 900	1.615	14 350	14 750	1.028

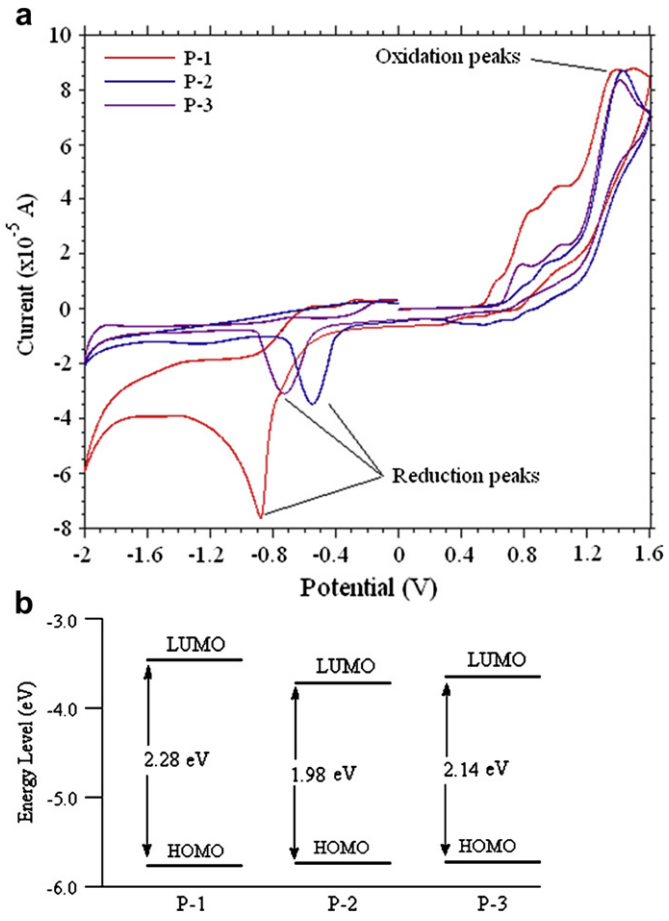

Fig. 4. Cyclic voltammograms of P-1, P-2, and P-3 (a) and schematic view of HOMO–LUMO energy levels and electrochemical band gaps (b).

P-3, respectively, indicate the d → d′ electron transitions of Cr(III). Also, the red shift in the UV–vis spectra of the polymers relative to monomeric model compound (3,4-HBA-Cr) is the evidence of the polyconjugated structures of the polymers. The absorption spectra are shown in Fig. 5. According to these spectra the optical band gap values (E_g) were calculated from absorption edges as in the literature [28] and found to be 2.43, 2.09, and 2.34 eV for P-1, P-2, and P-3, respectively. Because of the polyconjugated structures the synthesized polymers have quite lower band gaps and these values are sufficient to make these polymers electro-conductive materials.

The order of the optical band gap values is also agreement of the electrochemical band gap results. So on, P-2, with highly lower band gap value, has potential use in optical, electronic, and photovoltaic applications.

3.4. Doping procedure and electrical conductivities

Doping procedure of conducting polymers has attracted much attention of researchers into this field, so far [29]. This procedure

Table 3
Electronic structure parameters of the synthesized polymers.

Compounds	HOMO[a] (eV)	LUMO[b] (eV)	E_g[c] (eV)	E'_g[d] (eV)
P-1	−5.78	−3.50	2.43	2.28
P-2	−5.82	−3.84	2.09	1.98
P-3	−5.80	−3.66	2.34	2.14

[a] Highest occupied molecular orbital.
[b] Lowest unoccupied molecular orbital.
[c] Optical band gap.
[d] Electrochemical band gap.

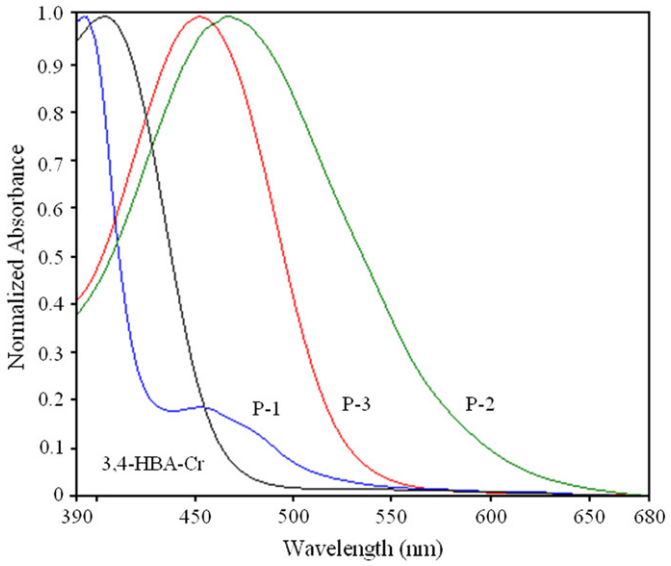

Fig. 5. Absorption spectra of 3,4-HBA-Cr, P-1, P-2, and P-3.

produces a lot of application fields for conducting polymers. With these properties conducting polymers are used in gas sensing materials as active layers [30,31]. For this aim, a lot of known conducting polymers such as polyaniline [32], polythiophene [33], polypyrrole [34] and their derivatives have been investigated as the gas sensors against several kinds of electro-donor (such as CO, CO_2, NH_3, H_2S, etc.) and electro-acceptor (such as I_2 and NO_2) gases. These studies show that the doping level and electrical conductivities of a conducting polymer can be changed considerable by doping with chemical vapors. The sensing mechanisms of these polymers have been also studied and much of them were clarified by electron transferring mechanism from and to the analytes [35]. Electron transferring causes changes in resistance and work function (W_f) of a conducting polymer. Conductivity and doping mechanisms of PAMs were also previously investigated by Diaz et al. According to the proposed mechanism, nitrogen is a very electronegative element and it is capable of coordinating an iodine molecule [36]. Schematic illustration of doping procedure and the possible doping reaction of P-1 are displayed in Fig. 6, as suggested in the literature [7,25].

Electrical conductivities of the synthesized polymers were determined as a function of temperature and doping time with iodine. The changes of conductivities related to these factors are shown in Fig. 7. As seen in Fig. 7a, the conductivity of undoped P-1 changed only a little with increasing the temperature. However, when it was doped with iodine vapor its conductivity increases with increasing the temperature between 40 and 70 °C. With iodine doping, the conductivity of P-1 increases by about 25 times of undoped state's conductivity at 70 °C and only one order of magnitude at 20 °C. Also, as seen in Fig. 7b, P-2 is the most electro-conductive polymer among the synthesized in both doped and undoped states. Additionally, when P-2 and P-3 doped with iodine for 24 h, their conductivities increase nearly 812 and 139 times of their initials, respectively. The increasing conductivity could indicate that a charge-transfer complex between the polymers and dopant iodine is continuously formed. Consequently, Fig. 7b not only shows the conductivity/doping time relationship but also indicate how quickly the doping reaction takes place. The experimental results show that a longer doping time is needed to obtain the maximal conductivity. As a result, the conductivity/doping time curves vary with doping conditions. As seen in Fig. 7c and d,

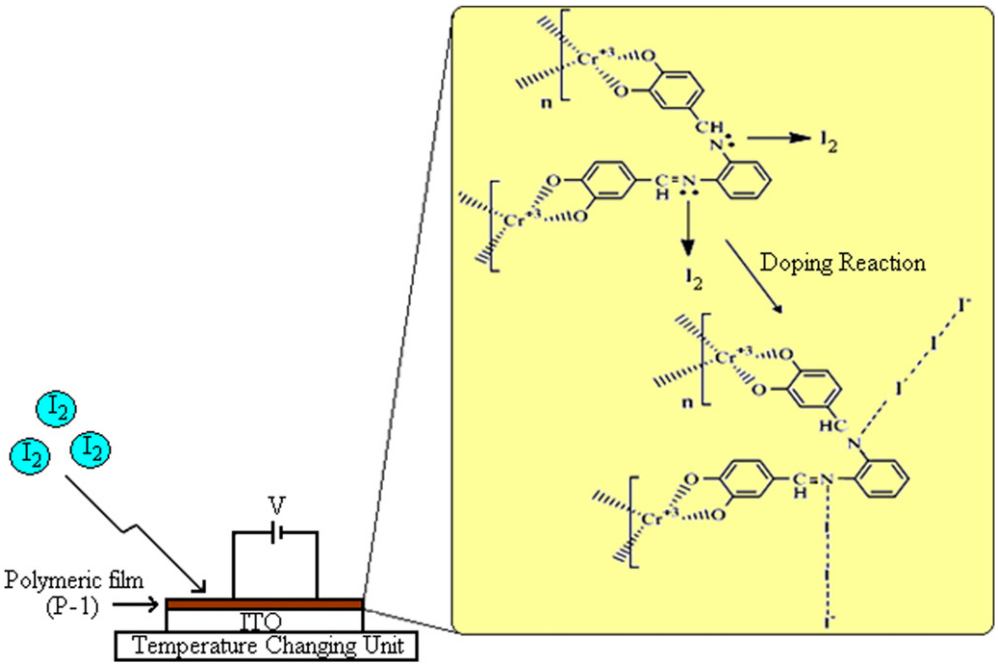

Fig. 6. Schematic illustration of doping procedure and the possible doping reaction of P-1.

undoped P-2 keeps its conductivity until 60 °C, but when the temperature increases to 70 °C, its conductivity increases by about two times of initial. However, it is seen that its conductivity changes only a little with increasing temperature, at the doped state. Obtained results clearly indicate that the order of conductivities of the synthesized polymers changes as P-2 > P-3 > P-1 for both doped and undoped states. These results also agree with the optical and electrochemical band gap values; lower band gap makes a polymer more electro-conductive.

Also, work function (W_f) of a polymer is defined as the minimal energy needed to remove an electron from bulk to vacuum energy level. This value can be estimated from absorption edges [37]. The changes in W_f (ΔW_f), therefore, can be evaluated from the difference between E_g values of doped and undoped states of the polymer. Fig. 8a and b show the absorption spectra of P-1 before and after doping and the absorption spectra of P-2 and P-3 after doping, respectively. As compared these spectra ΔW_f values (ΔW_{f1}, ΔW_{f2} and ΔW_{f3} for P-1, P-2 and P-3, respectively) of the polymers change

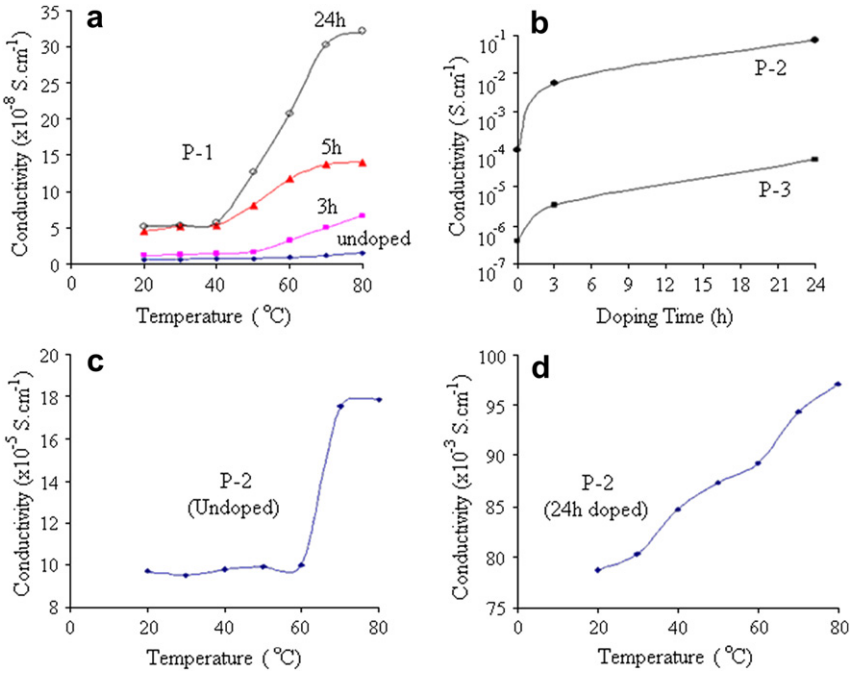

Fig. 7. The changes of conductivities of P-1 vs. temperature and doping time (a), P-2 and P-3 vs. doping time at 20 °C (b), undoped P-2 vs. temperature (c) and P-2 vs. temperature after 24 h doping (d).

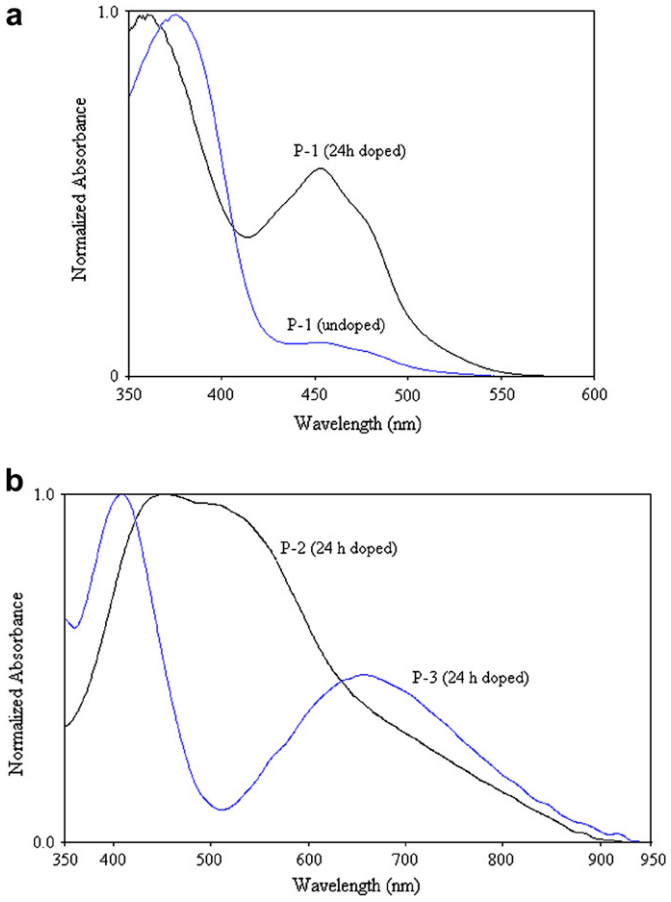

Fig. 8. The effect of doping procedure on the absorption spectra of the polymers: (a) The absorption spectra of doped and undoped states of P-1, (b) the absorption spectra of doped states of P-2 and P-3.

as follow: $\Delta W_{f3} > \Delta W_{f2} > \Delta W_{f1}$. Consequently, with regarding their quite low response time and ΔW_f values P-2 and P-3 can be used as active layers in gas sensors against electro-acceptor gases such as iodine.

3.5. Thermal analysis

TGA, DTG, DTA, and DSC analyses results of P-1, P-2, and P-3 are summarized in Table 4. As seen in Table 4, the initial degradation temperature (°C) and the carbon residue (%) at 1000 °C are 300 and 28 for P-1, 212 and 16 for P-2, and 187 and 9 for P-3. However, the synthesized polymers have absorbed and hydrate water in their structures, as mentioned in FT-IR analyses results. As determined from TG–DTG analysis of P-1, 22.66% weight loses between 40 and 243 °C can be attributed to absorbed and hydrate water removal. Also, 15% weight loses of P-2 between 40 and 160 °C and 12.15% weight loses of P-3 between 40 and 135 °C can be attributed to absorbed water removal [38]. As seen in the thermal degradation values, P-1 is the most thermally stable polymer among the synthesized. The order of thermal stabilities as follows: P-1 > P-2 > P-3. As seen in Table 4, any exo peak isn't observed in DTA curves. The presence of absorbed water is also confirmed by endothermic broad peaks between 40 and 200 °C, in DSC curves. The other endothermic peaks obtained in DSC analyses are also observed at 337 and 372 °C for P-1, 284 °C for P-2, and 285 °C for P-3. Additionally, T_g values of the polymers are determined and found to be 257, 264, and 237 °C for P-1, P-2, and P-3, respectively.

Table 4
Thermal degradation values of the synthesized chelate polymers.

Compounds	TGA					DTA		DSC	
	T_{on}[a]	W_{max}[b]	20% weight losses	50% weight losses	% Carbon residue at 1000 °C	Exo	Endo	T_g[c]	ΔC_p[d]
P-1	300	376	225	402	28	–	337, 372	257	0.174
P-2	212	242, 431, 937	226	650	16	–	284	264	0.139
P-3	187	211, 895	196	453	9	–	285	237	0.293

[a] The onset temperature (°C).
[b] Maximum weight temperature (°C).
[c] Glass transition temperature (°C).
[d] Change of specific heat during glass transition (J/g °C).

4. Conclusions

Soluble kinds of semi-conducting chelate polymers having polyconjugated structures were synthesized. Cr(III) kind was chosen in synthesize to obtain higher solubility. Obtained polymers were investigated with their optical, electrochemical, and electrical properties. It was stressed that the polymers having lower optical and electrochemical band gaps (E_g and E'_g) have also higher conductivities, as expected. So on, P-2 is the most electro-conductive polymer related to the lowest band gap. Also, the effects of temperature and doping procedure on electrical conductivities were investigated and considerable increasing on the conductivity of P-2 was detected when it was doped with iodine. According to having low response time and highly ΔW_f value P-2 can be promising as active layer in gas sensors against electro-acceptor gases, such as iodine. Thermal analysis results also showed that P-1 is the most thermally stable polymer among the synthesized, while it had high percentage of absorbed/hydrate water. Consequently, the synthesized chelate polymers are easy to process due to their high solubilities and with their polyconjugated structures they can be used in optical, electrochemical, electrical, photovoltaic applications, and gas sensing materials.

Acknowledgement

The authors thank TUBİTAK Grants Commission for a research grant (Project No: TBAG-107T414).

References

[1] Marvel CS, Bonsignore PV. J Am Chem Soc 1959;81:2668.
[2] Marin L, Cozan V, Bruma M, Grigoras VC. Eur Polym J 2006;42:1173–82.
[3] Grigoras M, Catanescu CO. J Macromol Sci Part C Polym Rev 2004;44:131–73.
[4] Kaya İ, Çulhaoğlu S, Gül M. Synth Met 2006;156(16–17):1123–32.
[5] Kaya İ, Demir HO, Vilayetoğlu AR. Synth Met 2002;126:183–91.
[6] Kaya İ, Yıldırım M. Eur Polym J 2007;43:127–38.
[7] Kaya İ, Yıldırım M. J Appl Polym Sci 2007;106:2282–9.
[8] Kaya İ, Bilici A. J Appl Polym Sci 2007;104:3417–26.
[9] Takahashi S, Morimoto H, Takai Y, Sonogashira K, Hagihara N. Mol Cryst Liq Cryst 1981;72:101–5.
[10] Zuo F, Yu I, Salmon MB, Hong X, Stupp SI. J Appl Phys 1991;69:7951–3.
[11] Kelch S, Rehahn M. Macromolecules 1999;32:5818–28.
[12] Kelch S, Rehahn M. Macromolecules 1997;30:6185–93.
[13] Holliday BJ, Stanford TB, Swager TM. Chem Mater 2006;18:5649–51.
[14] Whittell GR, Manners I. Adv Mater 2007;19:3439–68.
[15] Archer RD. Coord Chem Rev 1993;128:49–68.
[16] Kaya I, Yıldırım M. J Appl Polym Sci 2008;110:539–49.
[17] Kaya İ, Bilici A, Gül M. Polym Adv Technol 2008;19(9):1154–63.
[18] Kaya İ, Baycan F. Synth Met 2007;157:659–69.
[19] Kaya İ, Çetiner A, Saçak M. J Macromol Sci A 2007;44:463–8.
[20] Hirao T, Higuchi M, Yamaguchi S. Macromol Symp 1998;131:59–68.
[21] Walters KA, Ley KD, Cavalaheiro CSP, Miller SE, Gosztola D, Wasielewski MR, et al. J Am Chem Soc 2001;123:8329–42.
[22] Wong WY. J Inorg Organomet Polym 2005;15:197–219.

[23] Wolf MO. J Inorg Organomet Polym 2006;16:189–99.
[24] Marcos M, Oriol L, Serrano JL. Macromolecules 1992;25:5362–8.
[25] Kaya I, Yıldırım M. J Inorg Organomet Polym 2008;18:325–33.
[26] Ram MK, Joshi M, Mehrotra R, Dhawan SK, Chandra S. Thin Solid Films 1997;304:65–9.
[27] Cervini R, Li X-C, Spencer GWC, Holmes AB, Moratti SC, Friend RH. Synth Met 1997;84:359–60.
[28] Colladet K, Nicolas M, Goris L, Lutsen L, Vanderzande D. Thin Solid Films 2004;451:7–11.
[29] Lee KH, Ohshita J, Kunai A. Organometallics 2004;23:5365–71.
[30] Zakrzewska K. Thin Solid Films 2001;391:229–38.
[31] Timmer B, Olthuis W, van den Berg A. Sens Actuators B 2005;107:666–77.
[32] Agbor NE, Petty MC, Monkman AP. Sens Actuators B 1995;28:173–9.
[33] McCullough RD. Adv Mater 1998;10:93.
[34] Ruangchuay L, Sirivat A, Schwank J. React Funct Polym 2004;61:11–22.
[35] Bai H, Shi GQ. Sensors 2007;7:267–307.
[36] Diaz FR, Moreno J, Tagle LH, East GA, Radic D. Synth Met 1999;100:187–93.
[37] Blackwood D, Josowicz M. J Phys Chem 1991;95:493–502.
[38] Kaya I, Bilici A. J Macromol Sci A 2006;43:719–33.